# Exploring the effects of Compression via Principal Components Analysis on X-ray image classification

Vikash Rameshar, Wesley Doorsamy
Department of Electrical and Electronic Engineering Technology
University of Johannesburg
Johannesburg, South Africa
vikashr@uj.ac.za, wdoorsamy@uj.ac.za

Abstract—Image compression in medical applications implores careful consideration of the effects on data veracity. The inexorable challenge of assessing the volume-veracity trade-off is becoming more prevalent in this critical application area, and particularly when machine learning is used for the purpose of assisted diagnostics. This paper investigates the impact of compressing X-ray images on the accuracy of fracture diagnostics. The accuracy of the classification system is assessed for X-ray images of both healthy and fracture bones when subjected to different levels of compression. Compression is achieved using principal components analysis. Results indicate that accuracy is only marginally affected under a level one compression but begins to deteriorate under level two compression. These results are potentially useful as the level one compression yields gains up to 94% with less than a 2% drop in classification accuracy.

Index Terms—X-ray, image classification, principal component analysis, compression, big data

## I. Introduction

Medical imaging is amongst the most rapidly developing fields providing tremendous breakthroughs in medical research and clinical diagnosis [1]. In general, a foremost consideration in modern imaging is the data size or volume, which affects the storage and transmission bandwidth, and processing speed [1], [2]. Therefore, in order to meet the transmission, processing and storage requirements for the application, compression of the images is typically required. Since the application area of medical imaging is so critical, the compression of the images should not affect the quality so as to compromise the clinical diagnosis.

In this work, the effect of principal components analysis (PCA) -based compression of X-ray images on the performance of a fracture classification system is investigated. PCA enables redundant or insignificant image components to be excluded, thereby resulting in both, a suitable compression ratio and adequate quality for classification, after construction. The change in the performance of the classification system is assessed under varying levels of compression - i.e. varying levels of principal components

## II. Background

### A. X-ray Image Classification and Fracture Diagnosis

Image processing techniques are applied to various fields like space programs, aerial and satellite imagery as well as medicine [3]. Medical imaging is a set of digital image processing techniques that create and analyse X-ray images of the human body that make it possible for doctors, radiologist and medical scientists to examine [4]. Within the medical field, images are used for planning surgeries; X-ray imaging is used in finding bone deformities; Magnetic Resonance Imaging (MRI) is used to determine which layer of soft tissue and bone is affected [5]. The use of X-ray's in image processing is based on many factors that include cost and complexity when compared to MRI, PET (Positron Emission Tomography), CT images. X-ray images are also a preferred source to many classifiers within the computer vision industry. Image-guided interventions are a current technology that allows not only diagnoses but conducting treatment strategies and planning for surgeries [6]. MRI together with image guidance technology makes a difference in the removal of invasive cancers within the breast tissue of humans [6], [7]. The finding of multiple cancers in the same breast has been successfully detected using MRI technology [8]. Other cancers can be detected at its earliest stages due to Optical-based cellular imaging. PET imaging and MRI has also resulted in advancements in cancer detection [6], [8]. CT scans and MRI have been utilised in guided cardiovascular interventions allowing doctors to view arteries in 3D to find an obstruction [6], [7]. Ultrafast CT scanning allows the heart and coronary artery to be imaged and to guide cardiac procedures. An overview of the steps involved in a typical medical image processing and classification system is given in figure 1.

### B. Volume, Veracity and Value

The medical industry, amongst many others, is especially prone to Big Data. This is because medical data – particularly medical imaging data - is both voluminous, come from various sources, and are of tremendous value. In this paper, the issues of volume, veracity and value are considered. In X-ray imaging, the value and veracity of the data is critical towards correct diagnosis and is of obvious value. Fracture classification systems that process X-ray images to assist with diagnosis need to provide high levels of certainty. On the other hand, transfer, storage and processing of voluminous image data is both cumbersome and costly. Therefore, the opportunity to reduce volume of X-ray images without comprising the veracity of the data is of value. This paper investigates how compression of X-ray images - via principal components analysis - affects the accuracy of a fracture classification system.

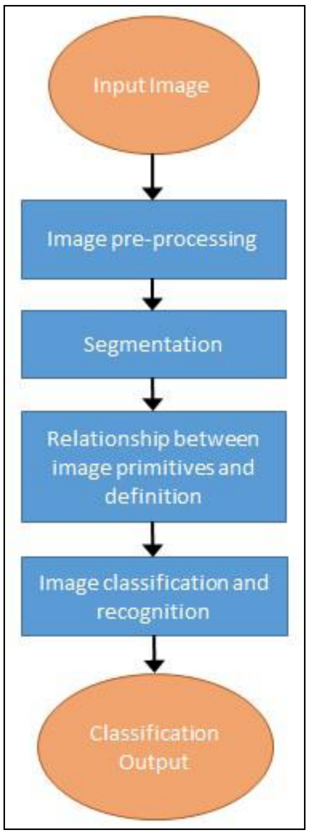


Fig.1: Process overview for typical X-ray image classification.

## III. METHODOLOGY

The focus of the presented investigation deals specifically with the assessment of compression effects on the classification accuracy. The classification system used in the investigation (shown in figure 2) is briefly described in the subsequent sections before the compression - as a pre-processing subsystem - is explained.

### *A. X-ray Image Classification System*

The complexity of the human body leads to the problem of determining the existence and location of possible fractures. Fractures range from compound to hairline, buckle to stress fractures. Most fractures that occur to the bones of the forearm are due to extra stress concentrated at a specific point [9], [10]. A fracture in most cases is referred to as a break in the bone material. Fracture severity can be challenging to determine as many fractures are not open wounds. Through the use of digital X-ray technology, this can now be exploited to detect fractures in the bone. Many Computational Intelligence Techniques such as Artificial Neural Networks, Support Vector Machines, and Fuzzy Inference Systems have been explored together with digital X-ray's to aid doctors in the diagnosis of fractures. Within the human forearm, two main bones are present namely the radius and ulna. When under tremendous stress, the ulna of the forearm is the most likely bone to fracture. In most cases, a fracture is most likely to occur at the mid-ulna of the forearm which was taken into consideration when the classifier systems were explored [11]. The SVM and FIS classifiers were trained with the mid-ulna Region of Interest (ROI). Although X-ray images contain many feature data, interest typically concentrated towards the soft tissue, background, bone, and fracture. The similarity of the SVM network to the MLP and FIS networks is the input vector which is mapped to a class space allowing the proficiency of the regression and classification [12].

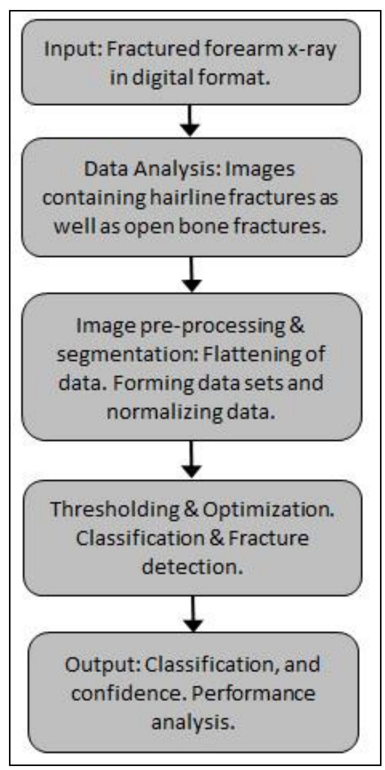


Fig. 2: Process overview for X-ray image classification and fracture detection system

*1)* X-ray input and data analysis: The most conventional X-ray imaging - in most general healthcare facilities – utilises X-ray film. Some of the X-ray film data has to first be digitised. A digital X-ray scanner was utilised for creating the investigated dataset, taking into consideration the quality of the X-ray images were not compromised. The abovementioned digitising method also impacts on the quality of X-ray data obtained which includes the required radiologist's supervision and the type of machine that can produce a quality image. Digitised images comprise of 2D and 3D matrices which have intensity and amplitude values [13]. In most cases grayscale images are utilised within image processing, this allows pixels of varying shades from 0 being black and 1 being white and colour images having different shades of RGB values ranging from 0 to 255 [13].

*2)* Image pre-processing and segmentation: Digitisation of the image data was further processed into a 5x5 matrix and fed into the system by a 1x25 vector. This enhances accuracy in interpretation of the data by the various classifiers and ease of data transmission. The pre-processing subsystem/stage segments the image into specific regions or ROIs (as shown in figure 3) that consisted of background, soft tissue, and bone data [11].

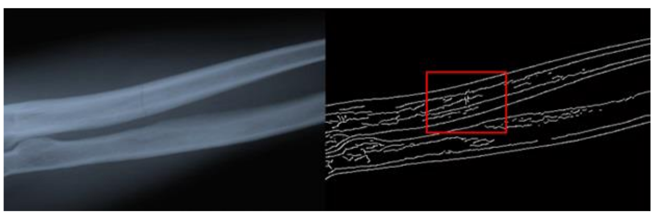

Fig. 3: Example of region of interest for segmentation

3) Classification and fracture detection: The segmentation of the X-ray images provided data that were utilised to classify the input data. Background, soft tissue and fractured bone data as well as normal bone data were utilized in training, validating and testing of the classification system. ANN, SVM and FIS classifiers predicted possible fractures when the X-ray images were propagated through the system [11].

4) Thresholding and optimisation: Due to the variance of pixels, threshold values -i.e. minimum and maximum values, are required. This can be achieved by automatically using a standised algorithm e.g. a genetic algorithm or by simply assigning minimum and maximum values. Minimum and maximum threshold values were set for the system which allowed for comparison of neighbouring pixels with similar contrast. This was further optimized using a genetic algorithm which utilized the scaled conjugate gradient (SCG) method. The method allowed for the minimisation of the error function within the ANN computation [11].

*B. Compression via Principal Components*

Compression of images are carried using a variety of different techniques inter alia removal of spectral redundancies, transform-based approaches, and PCA has been previously applied for compression in application areas such facial recognition and remote sensing [14], [15]. The approach taken here is to firstly separate the X-ray image in three colour schemes/components, and then perform PCA on these components. The proportion of variance is analysed to view the extent of contribution of the principal components on the overall image. The exclusion of principal components and subsequent reconstruction of the X-ray image constitutes the actual compression. Principal component Analysis of the X-ray images used in this investigation indicates that high proportions of variance are largely owing to approximately 30 principal components of the image. Simply put, this means that there is a possibility to exclude insignificant components without losing data that may be critical to classification. Examples of the proportion of variance plots obtained from PCA of an X-ray image used in this investigation are given in figures 5 and 6. The visual quality deterioration in the X-ray image after compression and reconstruction is given in figures 7a, 7b, and 7c.

*C. Image Preprocessing and Processing*

The approach taken here is to incorporate the compression via PCs as a pre-processing subsystem to the overall classification system shown in figure 2, in order to evaluate the effects of image compression. This modified system - with compression pre-processing - is shown in figure 4.

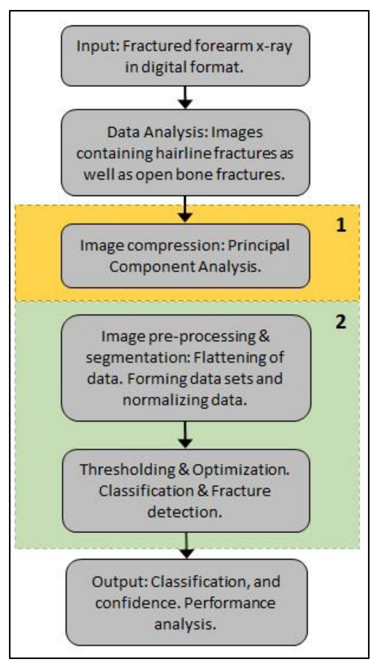


Fig. 4: Process overview for X-ray image classification and fracture detection system with modified compression preprocessing

It should be highlighted that only the SVM- and ANFIS-based classification systems are used in this investigation as focus is placed on the compression effects.

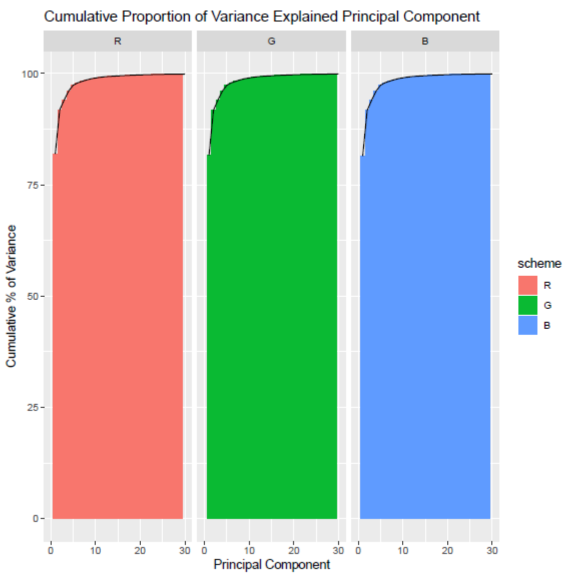


Fig. 5: Cumulative proportion of variance obtained from principal component analysis of X-ray image

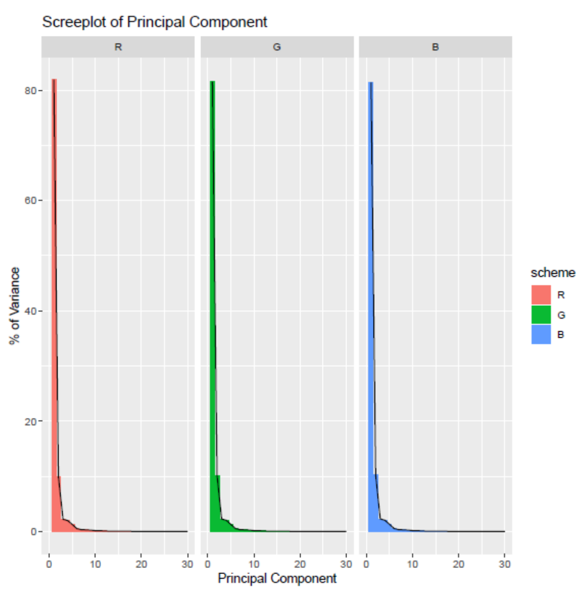


Fig. 6: Scree plot of variance obtained from principal component analysis of X-ray image

## IV. RESULTS AND ANALYSIS

### *A. Compression*

Two different levels of compression were applied consistently to all the images. For the level 1 compression, 200 components were extracted, while 30 components were extracted for level 2.

Although these compression levels are applied consistently, the resulting compression ratios and actual volumes for each of the X-rays are expectedly different due to variation in initial sizes. A summary of these results are given in table I.

TABLE I: Summary of size reductions resulting from different PCA compression levels

| Image | Level 1 (%) | Level 2 (%) |
| --- | --- | --- |
| H1 | 67.15174 | 69.1365 |
| H2 | 50.73583 | 64.50694 |
| H3 | 68.35623 | 74.20801 |
| H4 | 58.99052 | 63.80504 |
| H5 | 93.24539 | 93.30798 |
| F1 | 56.6188 | 57.25153 |
| F2 | 86.74174 | 87.64268 |
| F3 | 91.59408 | 91.67574 |
| F4 | 93.56891 | 93.57381 |
| F5 | 88.46931 | 89.09141 |


Fig. 7: X-ray image subjected to different compression rates (a) standard (uncompressed), (b) level 1 compression, and (c) level 2 compression.

### B. Classification Results

The compressed images were then put through the classification system, as shown in figure 4. The change in the classification accuracy for each of the classification system using the uncompressed X-ray images, and the X-rays compressed at the two different levels were recorded. Table II gives a summary of the decline in classification accuracies corresponding to each of the compressed images, where $\delta T_A(\%)$ corresponds to the normalised change in classification test accuracy using standard (uncompressed) X-ray image versus compressed X-ray image.

TABLE II: Summary of change (decrease) in classification accuracy for different levels of compression

| | $\delta T_A(\%)$ | | | $\delta T_A(\%)$ | |
|---|---|---|---|---|---|
| Image | ANFIS | SVM | Image | ANFIS | SVM |
| H1 (L1) | 3,05899 | 4,30538 | F1 (L1) | 1,24323 | 5,26247 |
| H1 (L2) | 12,11829 | 8,52315 | F1 (L2) | 11,23685 | 8,52206 |
| H2 (L1) | 0,11985 | 0,20720 | F2 (L1) | 0,62367 | 0,28612 |
| H2 (L2) | 2,15238 | 1,45535 | F2 (L2) | 2,82840 | 0,62947 |
| H3 (L1) | 38,02563 | 0,46695 | F3 (L1) | 37,13678 | 1,34590 |
| H3 (L2) | 48,61361 | 12,22659 | F3 (L2) | 47,68420 | 13,78931 |
| H4 (L1) | 0,78291 | 1,53117 | F4 (L1) | 2,88192 | 0,90425 |
| H4 (L2) | 9,53850 | 24,13416 | F4 (L2) | 8,81702 | 21,72674 |
| H5 (L1) | 0,43849 | 1,86494 | F5 (L1) | 3,15528 | 0,51013 |
| H5 (L2) | 24,56164 | 14,95026 | F5 (L2) | 25,16910 | 17,55136 |

## V. Conclusion

As medical imaging technology advances, so too does the need to account for the growing storage, transmission and processing bandwidth requirements. X-ray image-based classification systems for assisted fracture detection and diagnosis have become increasingly popular but suffer from the bottlenecks brought about by voluminous data. Thus, a compression technique that provides suitable ratios but does not adversely affect the performance of these classification systems is desired. The presented investigation deals with the assessment of PCA-based compression on the accuracy of an X-ray image classification system. A number of X-ray images are subjected to different levels of compression. The classifier system is applied to the normal and compressed images to determine changes in accuracy. Results indicate that, on average, a level 1 compression ratio diminishes the classification accuracy by approximately 8.75% (for ANFIS-based classification) and 1.67% (for SVM-based classification) while providing average compression ratios of approximately 75.7% for the test dataset. Although limited amount of X-ray image data were used, this study provides a clear case for further testing of PCA using a richer dataset. Furthermore, testing of X-ray images, done alongside diagnoses carried out by medical practitioners could bring out an understanding of the medical implications of the accuracy reductions of classification accuracies under varying levels of compression.

## References

[1] S. Liu, W. Bai, N. Zeng, and S. Wang, "A Fast Fractal Based Compression for MRI Images", *IEEE Access*, vol. 7, pp. 62412 - 62420, 2019.

[2] Z. Chen, H. Ye, and Z. Yingxue, "Effects of Compression on Remote Sensing Image Classification Based on Fractal Analysis", *IEEE Transactions on Geoscience and Remote Sensing*, vol. 57, no. 7, pp. 4577 - 4589, 2019.

[3] R. Gonzalez and R. E. Woods, *Digital image processing*, Prentice Hall, New Jersey, 2nd edition, 2002.

[4] T. W. Cai, J. Kim, and D. D. Feng, *"Content-based medical image retrieval"*, In David Dagan Feng (Ed.), *Biomedical information technology*, pp. 83-113, Burlington: Academic Press, 2008.

[5] S. Yadavalli, "Radiologic evaluation of musculoskeletal soft tissue infections: a pictorial review", *Current Radiology Reports*, vol. 3, no. 10, pp. 40, 2015.

[6] A. Greenspan, *Orthopedic Radiology*: *A Practical Approach*, Lippincott- Raven, Philadelphia, 2nd Edition, 1997.

[7] D. C. Cires¸an, A. Giusti, L. M. Gambardella, J. Schmidhuber, "Mitosis detection in breast cancer histology images with deep neural networks." *In International Conference on Medical Image Computing and Computer assisted Intervention*, Springer, Berlin, Heidelberg, pp. 411-418, 2013.

[8] F. Xing, Y. Xie, and L. Yang, "A Automatic Learning-Based Framework For Robust Nucleus Segmentation" *IEEE Transactions on Biomedical Imaging*, vol. 35, no. 2, pp. 550 – 66, 2015.

[9] M. P. Eiff, Hatch and W. L. Calmbach, "Radius and ulna fractures", *Fracture Management for Primary Care*, Philadelphia, Pa.: Saunders, 2nd ed., 2003.

[10] M. Bhandari, and E. H. Schemitsch, "Fractures of the shaft of the ulna", *Orthopedic Trauma*, vol. 18, no. 7, pp. 473–475, 2004.

[11] V. Rameshar, *X-ray Forearm Fracture Detection using Computational Intelligence Techniques*, Masters' thesis, University of Johannesburg, 2014.

[12] C. Cortes, and V. N. Vapnik, "Support-Vector Networks", *Machine Learning*, vol. 20, 1995.

[13] M. R. Razavi, *Characterization of Microstructure and internal Displacement Field of Sand using X-ray Computed Tomography*, Doctoral dissertation, Washington State University, 2006.

[14] L. Chulhee, S. Youn, T. Jeong, E. Lee, and J. Serra-Sagrist`a, "Hybrid compression of hyperspectral images based on PCA with pre-encoding discriminant information", *IEEE geoscience and remote sensing letters 12*, no. 7, pp. 1491 - 1495, 2015.

[15] S. Lihong, and C. Qiu. "Face Recognition by Feature Extraction and Classification", *In 2018 12th IEEE International Conference on Anticounterfeiting, Security, and Identification (ASID)*, pp. 43 - 46, 2018.